

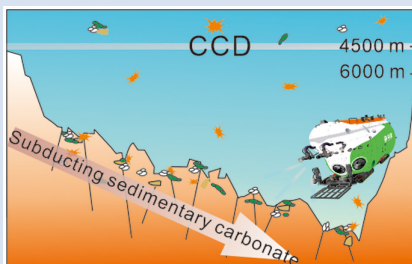
## Subduction of sedimentary carbonate in the Mariana trench

S. Liu<sup>1</sup>, X. Su<sup>2</sup>, S. Wan<sup>2</sup>, L. Zhang<sup>2</sup>, S. Chen<sup>1</sup>, W. Xu<sup>1</sup>, H. Xu<sup>1</sup>,  
D. Wang<sup>1</sup>, D. Li<sup>1</sup>, X. Peng<sup>1\*</sup>



<https://doi.org/10.7185/geochemlet.2425>

### Abstract



Calcium carbonate is a major component of shallow marine sediments but is rarely preserved in deep sea environments below the calcite compensation depth (CCD). In this study, we present evidence of sedimentary carbonate on the subducting Pacific plate of the Mariana Trench at a water depth ranging from 6675 to 10,813 m, far surpassing the local CCD of 4800 m. These deposits consist of well-preserved calcareous nannofossils, planktonic foraminifera, and siliceous radiolarians. Fossil assemblages and isotope stratigraphy analyses constrain the age of carbonate sediments to 17.6–13.5 Ma. We propose that the calcareous sediments originated from rapid deposition and burial on the seafloor above the CCD during the Miocene. Subsequently, they were transported into the hadal zone with the subduction of the Pacific Plate and

exposed due to the excavation of extensive subducting-related normal faults within the subducting plate. This study implies that sedimentary carbonate may be a key component of subducting carbon at the hadal subduction zones, which has important implications for evaluating global carbon input fluxes at these zones.

Received 24 January 2024 | Accepted 10 May 2024 | Published 26 June 2024

### Introduction

Calcite compensation depth (CCD) is a boundary in the ocean where the rate of calcium carbonate supply from the surface is matched by the dissolution. It forms the transition between carbonate-bearing and carbonate-absent zones and is thus linked to the ocean-atmosphere carbon cycling system and global climate (Van Andel, 1975; Rea and Lyle, 2005; Pälke *et al.*, 2012). At present, the CCD varies substantially with latitude and longitude and is estimated to be 4000–5000 m below sea level (msl) in the ocean (Sulpis *et al.*, 2018). In theory, the sediments below the CCD are essentially carbonate-free residues comprising sediments such as pelagic red clay and diatom ooze (Dutkiewicz and Müller, 2021).

The hadal zone, with depths greater than 6000 m, mostly comprised of deep trenches, and constituting the deepest part of the world's oceans, represents the least explored habitat. Tectonically, hadal trenches are formed in subduction zones and are thus key hinge points of the material cycling between the Earth's interior and exosphere (Du *et al.*, 2021). Subduction is the primary mechanism for transporting carbon from the surface into the interior of the Earth. Carbonate sediments, comprising up to 50 % of total carbon subduction fluxes, serve as the dominant host for carbon transported into the mantle at subduction zone settings (Plank and Manning, 2019). Nevertheless, carbonate sediment distribution exhibits significant spatial heterogeneity in global subduction zones (Kelemen and Manning, 2015; Clift, 2017). Traditionally, it was believed that carbonates would be completely absent in hadal sediments due to

the corrosive seawater. Previous studies thus proposed that no sedimentary carbon was subducted at hadal subduction zones, such as the Tonga, Central Aleutian, and Kuriles-Kamchatka Trenches (Rea and Ruff, 1996; Plank and Langmuir, 1998; Plank and Manning, 2019).

Here we provide the first study of carbonate deposits in the Mariana Trench (MT) from a water depth of 6675–10813 mbsl during an expedition in September 2021 with the manned submersible *Fendouzhe* (Fig. 1, Table S-1). The occurrence of sedimentary carbonate at hadal depths was unexpected, as it is far deeper than the CCD of this zone at 4800 mbsl. To elucidate this anomaly, we conducted morphological, mineralogical, and geochemical analyses, along with mode calculations, to explore the origin and unusual preservation of those carbonate sediments. Additionally, we established an age model using a combination of microfossil biostratigraphy and strontium/oxygen isotopes of the carbonate sediments.

### Results

The push-core from site FDZ050 is divided into two parts (Fig. 2e): the upper 0–3 cm is *in situ* pelagic brown clay sediments with low concentrations of siliceous radiolarians, and the lower 3–21 cm is mainly white biogenic deposits composing of well-preserved calcareous microfossils such as calcareous nannofossils, planktonic foraminifers, and dinoflagellates (Figs. 3, S-2 and S-3). Siliceous radiolarians are very abundant, with tens to hundreds of thousands of individuals *per* gram in the lower part (Fig. 3). The assemblages and distributions of marine microfossils in the lower

1. Institute of Deep-Sea Science and Engineering, Chinese Academy of Sciences, Sanya 572000, China

2. South China Sea Institute of Oceanology, Chinese Academy of Sciences, Guangzhou 510301, China

\* Corresponding author (email: [xpeng@idsse.ac.cn](mailto:xpeng@idsse.ac.cn))

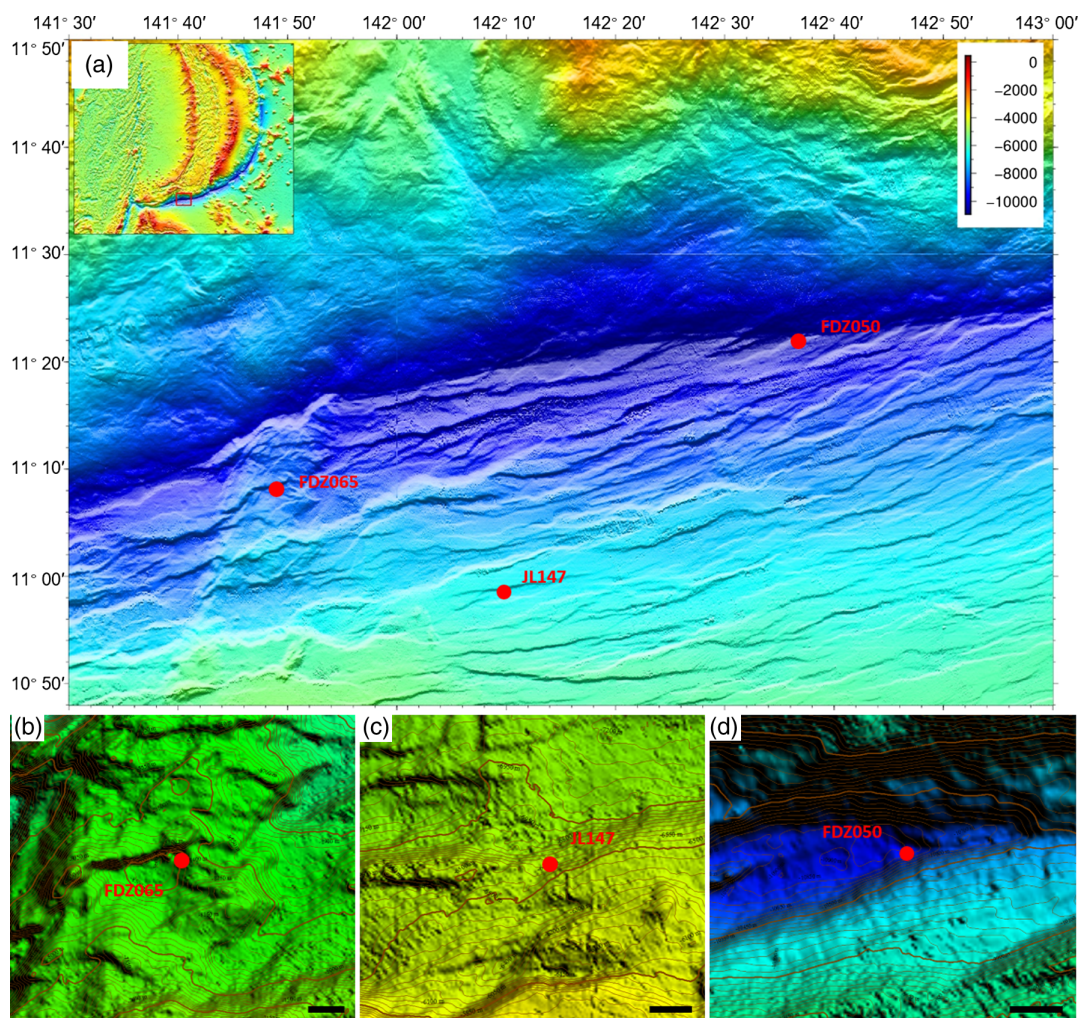


**Figure 1** (a) A bathymetric shaded relief map of the study area displaying the location of the discovered carbonate sediments (red dots) on the incoming Pacific plate of the Mariana Trench. The map was constructed using multi-beam data obtained during several visits to the area by the *R/V Tansuoyihao*. (b–d) Enlarged bathymetric maps show that the sites of carbonate sediments are closely associated with bending-related fault zones.

part of site FDZ050 are similar to those in the carbonate deposits at sites FDZ065 and JL147 (Fig. 3). Calcareous nannofossils are the most abundant microfossils in these carbonate deposits. The nannofossil assemblage is dominated by *Cyclicargolithus floridanus*, *Discoaster* spp, *Sphenolithus moriformis*, *Sphenolithus heteromorphus*, and *Reticulofenestra* spp (Table S-4, Figs. 3, S-2, S-3 and S-4). The carbonate deposits also include many planktonic foraminiferal tests, such as *Dentoglobigerina globularis* and *Globoturborotalita eua-pertura*, indicative of the early Miocene period (Fig. 3g–h). Based on the assemblages of marine microfossils and the presence of index fossils, the original deposit time is assigned to the Miocene between 17.6 and 13.5 Ma (Table S-4). The average  $^{87}\text{Sr}/^{86}\text{Sr}$  isotope ratio from four samples is 0.708477 (Table S-3). Comparison with the  $^{87}\text{Sr}/^{86}\text{Sr}$  ratio curves of McArthur *et al.* (2001) suggests an age of Miocene. Oxygen isotope values of carbonates (Table S-3) also further verify the sedimentary age of the Miocene (Grossman and Joachimski, 2020), which is consistent with the age suggested by the microfossil biostratigraphy.

XRD measurements and quantitative analysis suggest that the carbonate is calcite (Fig. S-1). Model calculations show that the sedimentary environments in hadal zones are under saturated with calcite and aragonite (Table S-2), indicating that the carbonate sediments can only survive under specific conditions. This result was further verified by the absence of carbonate

components in the other cores (Liu and Peng, 2019). Stable carbon isotope records of bulk sediments at Sites FDZ050 and 065 exhibit similar patterns (Table S-3).

## Discussion

**Potential genesis of carbonate deposits.** The absence of carbonate components in the upper 0–3 cm from site FDZ050 suggests that continuous carbonate deposition from the surface ocean was insufficient to counteract carbonate dissolution in the hadal environment. Consequently, these carbonate sediments are likely not the result of *in situ* deposits in the hadal settings.

A limited number of studies have reported the occurrence of carbonate deposits on the seafloor deeper than the modern CCD. For example, calcareous ooze sediments were discovered by the Ocean Discovery Program in the central basin of the South China Sea (Site U1433, 4372 m water depth, CCD at ~3500 m) (Zhou *et al.*, 2019), the North Pacific Ocean (Site 1179, 5565 m water depth, CCD at ~4500 m) (McCarthy *et al.*, 2004), and the East Pacific Rise (Site 1215, 5396 m water depth) (Leon-Rodriguez and Dickens, 2010). Calcareous deposits from sites U1433 and 1215 were interpreted as turbidity currents derived from adjacent carbonate platforms. In contrast, calcium carbonate at site 1179 was considered as a combined result of

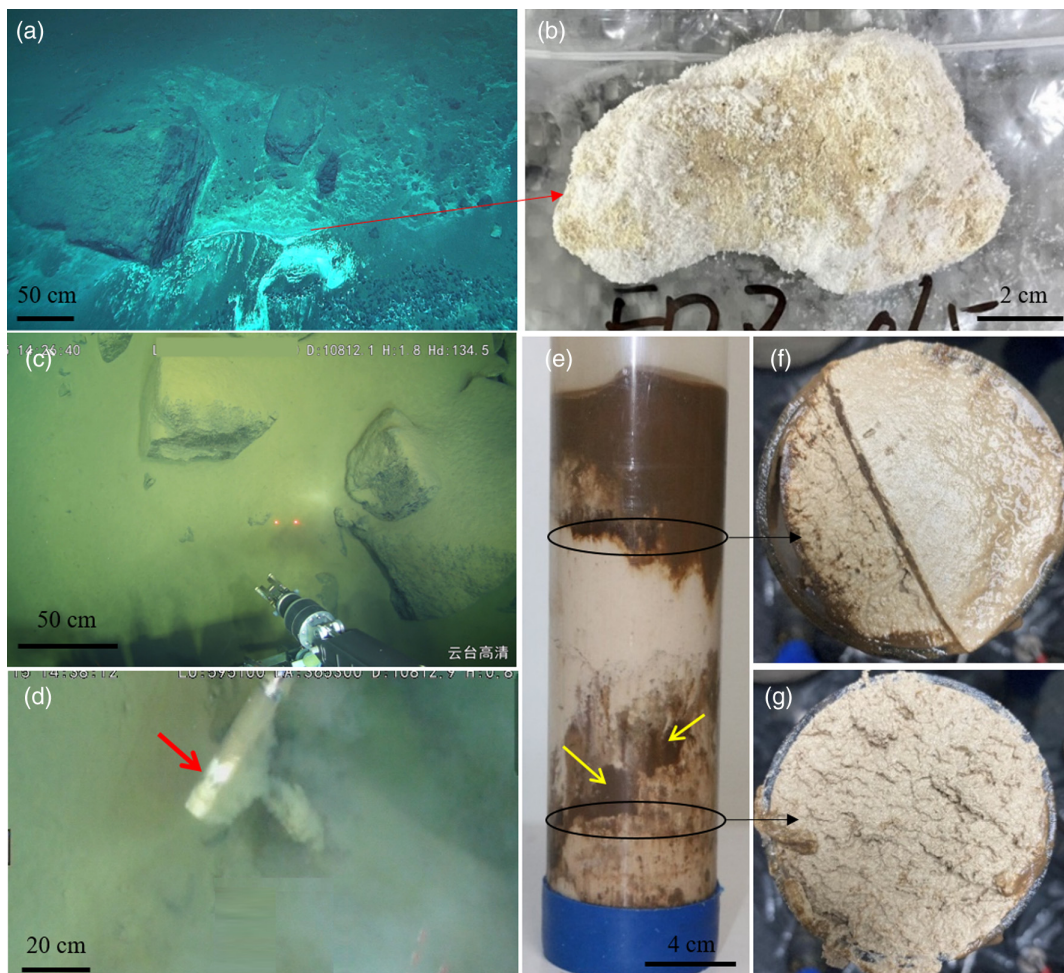


**Figure 2** Carbonate sediments in the Challenger Deep of the MT. (a) Outcrop of carbonate deposits at site FDZ065. (b) Carbonate specimen from site FDZ065. (c) Topographic feature showing the discovery of carbonate deposits at site FDZ050. (d) White materials marked by red arrow are carbonate sediments at site FDZ050. (e) Push-core sediments from site FDZ050. Note: the presence of deep sea clay around the lower part (indicated by yellow arrows) is a result of sampling artifacts that occurred during the insertion of the push-core. This is verified by the cross section of the push-core (f and g). The inner of the push-core is pure white without clay (f and g). Only the core samples were used for analysis in this study.

increased production of calcareous plankton at the sea surface and the rate of sedimentation to the seafloor. Furthermore, Yamamoto *et al.* (1988) reported carbonate turbiditic deposits at the Palau Trench at 8053 m, while carbonate-rich sediments were also found at the New Britain Trench at 8225 m (Luo *et al.*, 2019). These deposits were generally attributed to rapid deposition and burial resulting from recent mass wasting events.

A prominent feature of the hadal zone is the frequent occurrence of sediment mass wasting events (Zabel *et al.*, 2022). These events, often triggered by common earthquakes, can rapidly transport material from shallow water into the hadal zone, which could potentially explain the origin of carbonate sediments in this study as frequent slump deposits. However, we exclude mass wasting deposits based on the following evidence: (1) current research indicates that mass wasting events primarily occur on the landward slope (overlying plate) of hadal trenches, such as the Middle America Trench (Ranero and von Huene, 2000) and the Japan Trench (McHugh *et al.*, 2016). The steeper topography of the overlying plate favours sediment transport into the hadal zone through mass wasting events (Ueda *et al.*, 2023). (2) The majority of bending-related normal faults, located in the subducting plate of the hadal trenches (Ranero *et al.*, 2003; Zhou *et al.*, 2015), give rise to abundant horst structures reaching heights of up to 400 m. These structures

impede sediment transport from shallow water to the hadal trench through mass wasting events (Fig. S-5). In contrast, sediments can be transported into the hadal zone on the landward slope *via* mass wasting events (McHugh *et al.*, 2016). (3) The well preserved morphology of calcareous nannofossils, including intact coccolithophores (Fig. 3), suggests that they were not subjected to harsh transport processes such as debris flow or turbidity. Submarine channels (such as valleys or canyons), necessary for turbidity formation, have not been identified in the Challenger Deep through new high resolution multibeam mappings (Figs. 1, S-5). These carbonate deposits, characterised by abundant calcareous microfossils and a complete absence of mud or clay matrix, clearly result from rapid *in situ* deposits of calcareous fossils. If these carbonate sediments were transported to the hadal zone by turbidity currents, they would be exposed to corrosive seawater, leading to widespread dissolution. Figure S-4 shows that sedimentary carbonate dissolution occurred at a depth of 4 cm, not 21 cm, further excluding the possibility of turbidity current genesis. In summary, our study convincingly refutes the turbidity genesis hypothesis.

Previous studies suggest that the time before burial of calcareous microfossils in sediments below the CCD far exceeds their complete dissolution time (Honjo and Erez, 1978). Additionally, calcareous nannofossils do not show evidence of

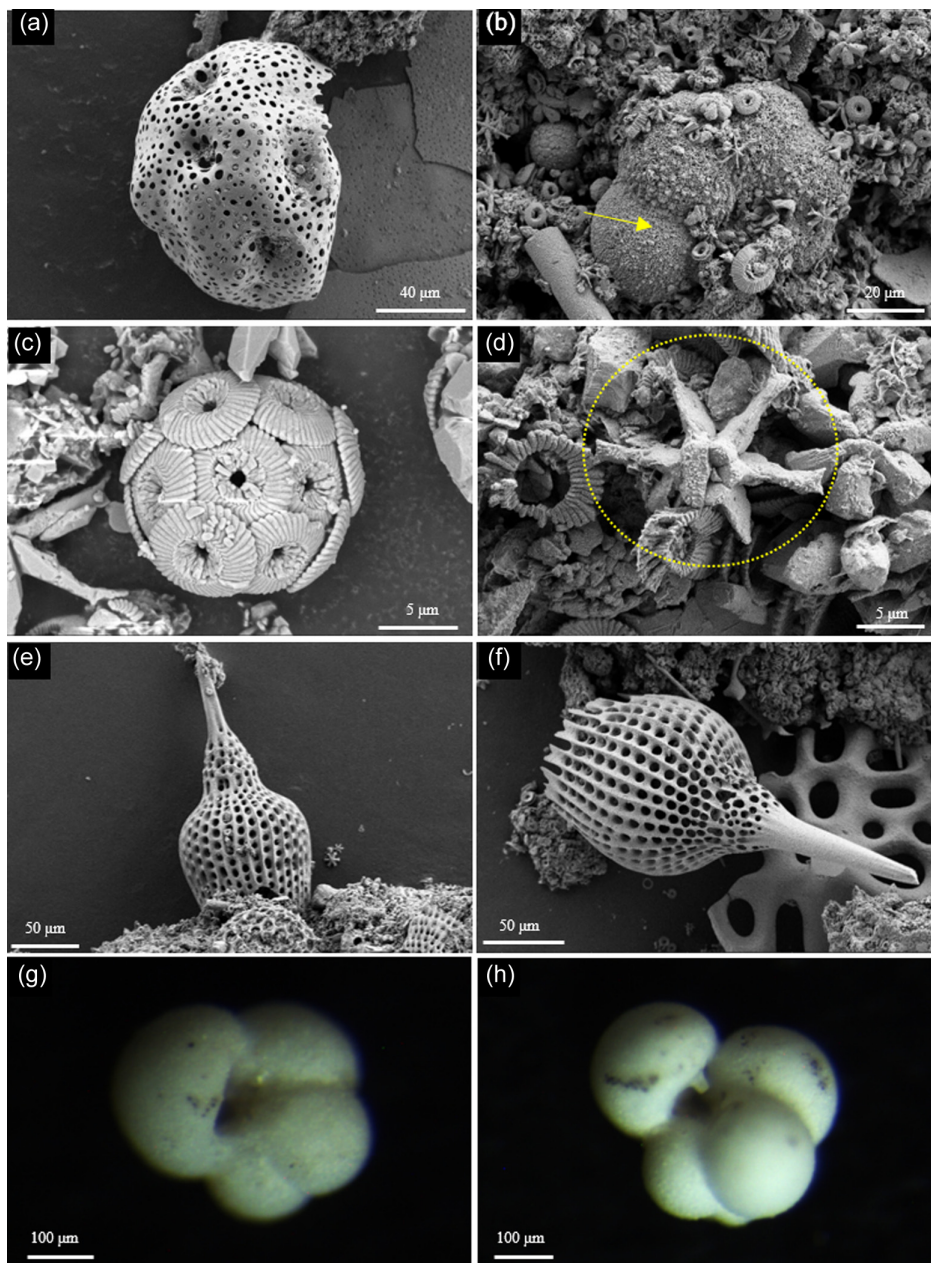


**Figure 3** Photomicrographs of carbonate sediments from the studied samples. (a) *Buccinosphaera invaginata*, First Appearance Datum (FAD): 0.34 Ma, 2 cm depth at site FDZ050. (b) *Paragloborotalia siakensis*, age: lower Oligocene–upper Miocene, 8 cm depth at FDZ050. (c) *Cycliscardolites floridanus*, age: Paleogene 11.85 Ma, 8 cm depth at FDZ050. (d) *Discoaster exilis*, age: 17.39–10.49 Ma, 8 cm of FDZ050. (e) *Calocycletta mizutamiensis*, age: early mid-Miocene, 8 cm depth at FDZ050. (f) *Calocycletta costata*, age: 17.6–13.44 Ma, 21 cm depth at FDZ050. (g) Planktonic foraminifera *Globoturborotalita euapertura*, age: Oligocene–early Miocene, FDZ065. (h) Planktonic foraminifera *Dentoglobigerina globularis*, age: Oligocene–early Miocene, FDZ065.

intense dissolution (Figs. 3, S-4b), suggesting that those carbonates were not exposed in hadal environments for a long period. This implies that the explanation of increased production of calcareous plankton at the sea surface and an increased rate of sedimentation on the seafloor may not apply here.

The geomorphic settings of the studied sites share similarities, being located on normal faulting scarps in the subducting plate (Figs. 1, S-5), implying a potential correlation between the outcropping of carbonate sediments and these faults. Bending-related extensional faults extensively traverse the entire trench slope of the subducting Pacific plate in the MT (Zhou *et al.*, 2015). The development of these extensional bending-related faults favours the exhumation of deeply buried carbonate

sediments. The absence of carbonate components in nearby cores located in graben zones (Liu and Peng, 2019) further supports the idea that the exposure of carbonate sediment is related to subducting-related normal faults.

In summary, we propose a three stage model as a potential genesis for the carbonate deposits in the MT (Fig. 4): (1) carbonate materials from the surface ocean were rapidly deposited and buried in the seafloor above the CCD during the early–middle Miocene, (2) the subduction of the Pacific plate transported these carbonate sediments from the sedimentation site to the Challenger Deep of the MT, and (3) carbonate sediments were exposed due to the subducting-related normal faults. While another explanation could be the deepening of the CCD in

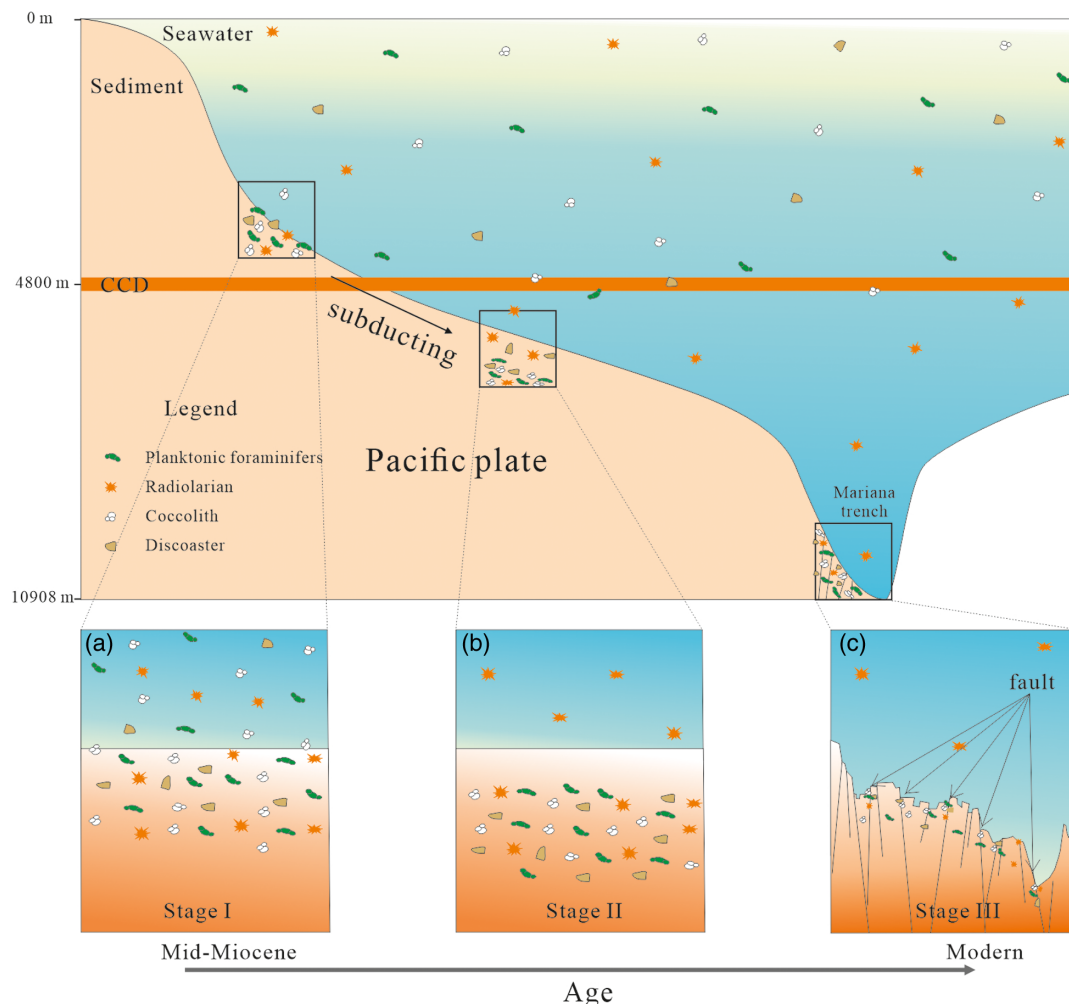


**Figure 4** Conceptual diagram depicting the potential genesis of carbonate sediments in the Challenger Deep of the MT. **(a)** Stage I: carbonate was rapidly deposited and buried in the seafloor above the CCD during the mid-Miocene. **(b)** Stage II: the Pacific plate subduction carried these carbonate sediments from the site of sedimentation to the Challenger Deep of the MT. **(c)** Stage III: carbonate sediments were exposed due to the subducting-related normal faults.

the geological evolution of oceans leading to carbonate deposits in hadal zones, we consider this highly unlikely, as it was improbable that CCD fluctuation exceeded 1 km at the equatorial Pacific since the Miocene (Pälike *et al.*, 2012).

**Implications for subducting carbon.** Sedimentary carbonates were considered to contribute approximately 80 % of the total subducting carbon sediment flux (Clift, 2017). However, they are rare on the seafloor near hadal trenches, such as the Mariana and Tonga trenches, resulting in essentially zero sedimentary carbonate being subducted along these old and cold oceanic plates (Plank and Manning, 2019). The Mariana subduction system, characterised as a non-accretionary convergent plate margin (Haggerty, 1991), indicates that all the sediments reaching the trench are ultimately subducted into the mantle (Plank and Langmuir, 1993; Fryer *et al.*, 2020). ODP sites 800 and 801 on the subducting Pacific plate have revealed a few calcareous-rich sedimentary layers containing shallow water carbonate debris or nannofossils at Paleocene and Cretaceous intervals (Rea and Ruff, 1996; Plank and Langmuir, 1998). However, these sites are located farther away from the MT, exceeding approximately 600 km from the MT axis. Sedimentary components at these sites may be significantly affected by long distance transport by the plate and may not entirely represent sediments subducting beneath the MT. The

occurrence of carbonate sediments in the Challenger Deep provides unambiguous evidence that carbon can indeed subduct into the MT in the form of sedimentary carbonates. Therefore, carbonate sediments contribute to the carbon source in the deepest subduction zone.

With sedimentary carbonate identified as a carrier of carbon into the mantle under the MT, we estimated a total carbon content in sedimentary carbonates of at least 2.49 million tons (Mt) at the Challenger Deep (see method in SI). Extrapolating this content to the entire 1400 km length of the MT, with a subduction rate of 4.75 km/Ma (Plank and Langmuir, 1998), reveals that approximately  $68.4 \times 10^4$  Mt/Ma carbon in the form of sedimentary carbonates are subducted into MT. Despite large errors, this flux far exceeds the previously estimated carbon input flux into the MT (Clift, 2017). Additionally, carbonate deposits were found at three dives, accounting for ~10 % of total dives during the TS21 cruise. This implies that carbonate sediments may be more spatially extensive in the Challenger Deep of the MT than we initially observed during the TS21 cruise. We therefore propose that sedimentary carbonate may represent a non-negligible component of the carbon input flux in the hadal subduction zones. Further dives are necessary to assess the abundance and distribution of carbonate sediments in the global hadal subduction zones.

## Acknowledgements

We are thankful to the crews of the R/V Tan Suo Yi Hao for their help during the Expedition. This study was financially supported by the National Key R&D Program of China (Grant No. 2022YFC2805400), the Hadal Science and Technology Program (Grant No.183446KYSB20210002), Youth Talent Fund from the Chinese Academy of Sciences Guangzhou Branch and the Guangdong Basic and Applied Basic Research Foundation (Grant No.2023A1515011955). Editor Eric Oelkers and four anonymous reviewers are thanked for helpful comments that helped to improve the manuscript.

Editor: Eric H. Oelkers

## Additional Information

Supplementary Information accompanies this letter at <https://www.geochemicalperspectivesletters.org/article2425>.



© 2024 The Authors. This work is distributed under the Creative Commons Attribution Non-Commercial No-Derivatives 4.0

License, which permits unrestricted distribution provided the original author and source are credited. The material may not be adapted (remixed, transformed or built upon) or used for commercial purposes without written permission from the author. Additional information is available at <https://www.geochemicalperspectivesletters.org/copyright-and-permissions>.

**Cite this letter as:** Liu, S., Su, X., Wan, S., Zhang, L., Chen, S., Xu, W., Xu, H., Wang, D., Li, D., Peng, X. (2024) Subduction of sedimentary carbonate in the Mariana trench. *Geochem. Persp. Let.* 31, 8–13. <https://doi.org/10.7185/geochemlet.2425>

## References

- HAGGERTY, J.A. (1991) Evidence from fluid seeps atop serpentine seamounts in the Mariana forearc: Clues for emplacement of the seamounts and their relationship to forearc tectonics. *Marine Geology* 102, 293–309. [https://doi.org/10.1016/0025-3227\(91\)90013-T](https://doi.org/10.1016/0025-3227(91)90013-T)
- CLIFT, P.D. (2017) A revised budget for Cenozoic sedimentary carbon subduction. *Reviews of Geophysics* 55, 97–125. <https://doi.org/10.1002/2016RG000531>
- DU, M., PENG, X., ZHANG, H., YE, C., DASGUPTA, S., LI, J., LI, J., LIU, S., XU, H., CHEN, C., JING, H., XU, H., LIU, J., HE, S., HE, L., CAI, S., CHEN, S., TA, K. (2021) Geology, environment, and life in the deepest part of the world's oceans. *The Innovation* 2, 100109. <https://doi.org/10.1016/j.xinn.2021.100109>
- DUTKIEWICZ, A., MÜLLER, R.D. (2021) The carbonate compensation depth in the South Atlantic Ocean since the Late Cretaceous. *Geology* 49, 873–878. <https://doi.org/10.1130/G48404.1>
- FRYER, P., WHEAT, C.G., WILLIAMS, T., KELLEY, C., JOHNSON, K., *et al.* (2020) Mariana serpentinite mud volcanism exhumes subducted seamount materials: implications for the origin of life. *Philosophical Transactions of the Royal Society A* 378, 20180425. <https://doi.org/10.1098/rsta.2018.0425>
- GROSSMAN, E.L., JOACHIMSKI, M.M. (2020) Chapter 10 - Oxygen Isotope Stratigraphy. In: GRADSTEIN, F.M., OGG, J.G., SCHMITZ, M.D., OGG, G.M. (Eds.) *Geologic Time Scale 2020*. Elsevier, Amsterdam, 279–307. <https://doi.org/10.1016/B978-0-12-824360-2.00010-3>
- HONJO, S., EREZ, J. (1978) Dissolution rates of calcium carbonate in the deep ocean; an in-situ experiment in the North Atlantic Ocean. *Earth and Planetary Science Letters* 40, 287–300. [https://doi.org/10.1016/0012-821X\(78\)90099-7](https://doi.org/10.1016/0012-821X(78)90099-7)
- KELEMEN, P.B., MANNING, C.E. (2015) Reevaluating carbon fluxes in subduction zones, what goes down, mostly comes up. *Proceedings of the National Academy of Sciences* 112, E3997–E4006. <https://doi.org/10.1073/pnas.1507889112>
- LEON-RODRIGUEZ, L., DICKENS, G.R. (2010) Constraints on ocean acidification associated with rapid and massive carbon injections: The early Paleogene record at ocean drilling program site 1215, equatorial Pacific Ocean. *Palaeogeography, Palaeoclimatology, Palaeoecology* 298, 409–420. <https://doi.org/10.1016/j.palaeo.2010.10.029>
- LIU, S., PENG, X. (2019) Organic matter diagenesis in hadal setting: Insights from the pore-water geochemistry of the Mariana Trench sediments. *Deep-Sea Research Part I-Oceanographic Research Papers* 147, 22–31. <https://doi.org/10.1016/j.dsr.2019.03.011>
- LUO, M., GIESKES, J., CHEN, L., SCHOLTEN, J., PAN, B., LIN, G., CHEN, D. (2019) Sources, Degradation, and Transport of Organic Matter in the New Britain Shelf-Trench Continuum, Papua New Guinea. *Journal of Geophysical Research-Biogeosciences* 124, 1680–1695. <https://doi.org/10.1029/2018JG004691>
- MCCARTHUR, J.M., HOWARTH, R.J., BAILEY, T.R. (2001) Strontium isotope stratigraphy: LOWESS version 3: best fit to the marine Sr-isotope curve for 0–509 Ma and accompanying look-up table for deriving numerical age. *The Journal of Geology* 109, 155–170. <https://doi.org/10.1086/319243>
- MCCARTHY, F.M., FINDLAY, D.J., LITTLE, M.L. (2004) The micropaleontological character of anomalous calcareous sediments of late Pliocene through early Pleistocene age below the CCD in the northwestern North Pacific Ocean. *Palaeogeography, Palaeoclimatology, Palaeoecology* 215, 1–15. <https://doi.org/10.1016/j.palaeo.2004.07.032>
- MCHUGH, C.M., KANAMATSU, T., SEEBER, L., BOPP, R., CORMIER, M.-H., USAMI, K. (2016) Remobilization of surficial slope sediment triggered by the A.D. 2011 Mw9 Tohoku-Oki earthquake and tsunami along the Japan Trench. *Geology* 44, 391–394. <https://doi.org/10.1130/G37650.1>
- PÁLIKE, H., LYLE, M.W., NISHI, H., RAFFI, I., RIDGWELL, A., *et al.* (2012) A Cenozoic record of the equatorial Pacific carbonate compensation depth. *Nature* 488, 609–614. <https://doi.org/10.1038/nature11360>
- PLANK, T., LANGMUIR, C.H. (1993) Tracing trace elements from sediment input to volcanic output at subduction zones. *Nature* 362, 739–743. <https://doi.org/10.1038/362739a0>
- PLANK, T., LANGMUIR, C.H. (1998) The chemical composition of subducting sediment and its consequences for the crust and mantle. *Chemical Geology* 145, 325–394. [https://doi.org/10.1016/S0009-2541\(97\)00150-2](https://doi.org/10.1016/S0009-2541(97)00150-2)
- PLANK, T., MANNING, C.E. (2019) Subducting carbon. *Nature* 574, 343–352. <https://doi.org/10.1038/s41586-019-1643-z>
- RANERO, C.R., VON HUENE, R. (2000) Subduction erosion along the Middle America convergent margin. *Nature* 404, 748–752. <https://doi.org/10.1038/35008046>
- RANERO, C.R., MORGAN, J.P., MCINTOSH, K., REICHERT, C. (2003) Bending-related faulting and mantle serpentinization at the Middle America trench. *Nature* 425, 367–373. <https://doi.org/10.1038/nature01961>
- REA, D.K., LYLE, M.W. (2005) Paleogene calcite compensation depth in the eastern subtropical Pacific: Answers and questions. *Paleoceanography* 20. <https://doi.org/10.1029/2004PA001064>
- REA, D.K., RUFF, L.J. (1996) Composition and mass flux of sediment entering the world's subduction zones: Implications for global sediment budgets, great earthquakes, and volcanism. *Earth and Planetary Science Letters* 140, 1–12. [https://doi.org/10.1016/0012-821X\(96\)00036-2](https://doi.org/10.1016/0012-821X(96)00036-2)
- SULPIS, O., BOUDREAU, B.P., MUCCI, A., JENKINS, C., TROSSMAN, D.S., ARBIC, B.K., KEY, R.M. (2018) Current CaCO<sub>3</sub> dissolution at the seafloor caused by anthropogenic CO<sub>2</sub>. *Proceedings of the National Academy of Sciences* 115, 11700–11705. <https://doi.org/10.1073/pnas.1804250115>
- UEDA, H., KITAZATO, H., JAMIESON, A., BOND, T., CARDIGOS, S., FUNAKI, M., MARONI, P.J., NANBU, H., O'CALLAGHAN, J.M., ONISHI, T., PEDERSEN, S.W., ROPEREZ, J., TSURUZONO, H., WATANABE, H.K., YASUDA, T., PRESSURE DROP RING OF FIRE EXPEDITION JAPAN CRUISE LEG2 SCIENCE TEAM (2023) The submarine fault scarp of the 2011 Tohoku-oki Earthquake in the Japan Trench. *Communications Earth & Environment* 4, 476. <https://doi.org/10.1038/s43247-023-01118-4>
- VAN ANDEL, T.H. (1975) Mesozoic/cenozoic calcite compensation depth and the global distribution of calcareous sediments. *Earth and Planetary Science Letters* 26, 187–194. [https://doi.org/10.1016/0012-821X\(75\)90086-2](https://doi.org/10.1016/0012-821X(75)90086-2)
- YAMAMOTO, S., TOKUYAMA, H., FUJIOKA, K., TAKEUCHI, A., UJIE, H. (1988) Carbonate turbidites deposited on the floor of the Palau Trench. *Marine Geology* 82, 217–233. [https://doi.org/10.1016/0025-3227\(88\)90142-9](https://doi.org/10.1016/0025-3227(88)90142-9)
- ZABEL, M., GLUD, R.N., SANEL, H., ELVERT, M., PAPE, T., CHUANG, P.C., OKUMA, E., GEPRÄGS, P., KÖLLING, M. (2022) High Carbon Mineralization Rates in Subseafloor Hadal Sediments—Result of Frequent Mass Wasting. *Geochemistry, Geophysics, Geosystems* 23, e2022GC010502. <https://doi.org/10.1029/2022GC010502>
- ZHOU, X., LYU, X., LIU, C., LIU, Z., LI, Q., JIN, X., ZHANG, H., DADD, K. (2019) Depositional mechanisms for upper Miocene sediments in the South China Sea central basin: Evidence from calcareous nannofossils. *Marine Micropaleontology* 151, 101768. <https://doi.org/10.1016/j.marmicro.2019.101768>
- ZHOU, Z., LIN, J., BEHN, M.D., OLIVE, J.-A. (2015) Mechanism for normal faulting in the subducting plate at the Mariana Trench. *Geophysical Research Letters* 42, 4309–4317. <https://doi.org/10.1002/2015GL063917>